Appl. Phys. B 31, 157–161 (1983)

Applied Physics B Photophysics and Laser Chemistry

Kinetic Studies of Ar_2F^* in Fast Transverse-Discharge-Excited He–Ar–F_2 Mixtures

Gu Zhi-yu*, Wang Shao-yin*, D. Proch, F. Rebentrost, H. Weber, and K. L. Kompa

Max-Planck-Institut für Quantenoptik, D-8046 Garching bei München,
Fed. Rep. Germany

Received 9 March 1983/Accepted 16 March 1983

Abstract. Time-resolved and time-integrated spectra for various He–Ar–F_2 mixtures excited by a fast transverse discharge were recorded. The fluorescence of ArF* and Ar_2F^* was investigated and the radiative lifetime and emission characteristics of Ar_2F^* were determined. A mechanism for the formation of Ar_2F^* is suggested.

PACS: 42.55 H, 52.80

Rare-gas halide exciplex molecules which radiate from a strongly bound excited state to a repulsive ground state were first observed by Velazco and Setser [1, 2]. Detailed spectral and structural analysis studies as well as ab initio calculations were reported soon thereafter [3]. While these diatomic RgX* molecules were investigated, discovery of a new class of triatomic rare-gas halide exciplex molecules was made [4]. The broad-band continuum emissions of triatomic rare-gas halides were identified as transitions between ionically bound excited states ($Rg_2^+X^-$) and repulsive covalent lower states, that dissociate to ground state atoms [5].

The triatomic exciplex Ar_2F^* has a broad contiuum emission centered around 290 nm [6, 7]. It therefore merits consideration as a potential candidate for a widely tunable uv laser. Previously, the formation and decay processes of Ar_2F^* in Ar–F_2 and Ar–NF_3 mixtures were investigated by Nakano et al. [6], Lorents et al. [4], Marowsky et al. [8] using electron beam excitation, and by Chen and Payne [11] and Chen et al. [12] using proton beams. Böwering et al. [13] report on the kinetics of Ar_2F^* from e-beam excited Ar–NF_3 and He–Ar–NF_3 mixtures. Corresponding data obtained under conditions of direct electric discharge have not been published so far.

Discharge excitation is very attractive under two aspects:

1) Low energy electrons feature large excitation cross-sections, which translates to a high pumping efficiency [10].

2) High pulse repetition rates, that is high average laser powers, are possible. Understanding the kinetics initiated by a fast discharge is a prerequisite to evaluate the chances of a directly pumped Ar_2F^* laser and should thus be rewarding.

In this contribution we report on our investigation about the kinetics of He/Ar/F_2 mixtures excited by a TEA discharge. The partial pressures of the three gas components were varied, the ranges are given in Sect. 1. Since the electron temperature is lower in the discharge than under e-beam excitation conditions, a different reaction kinetics may be expected. Backed by experimental observations this paper suggests a scheme leading to the formation of Ar_2F^*. It also reports the radiative lifetime of this trimer and the rate constant for quenching by F_2.

1. Experimental

The experimental setup is shown in Fig. 1. A detailed description of the fast TEA discharge can be found elsewhere [14]. A main capacitor (200 nF) charged to 36 kV resonantly charges 40 nF capacitors to produce a fast discharge. The pump power density is estimated to be about 30 MW/cm^3. Laser gases are premixed in a circulation system before being admitted to the discharge chamber. Partial and total pressures are measured by a capacitance gauge (MKS Baratron, Model 170 M-26 B).

---

* Permanent address: Academia Sinica, Institute of Optics and Fine Mechanics, Hofei, China

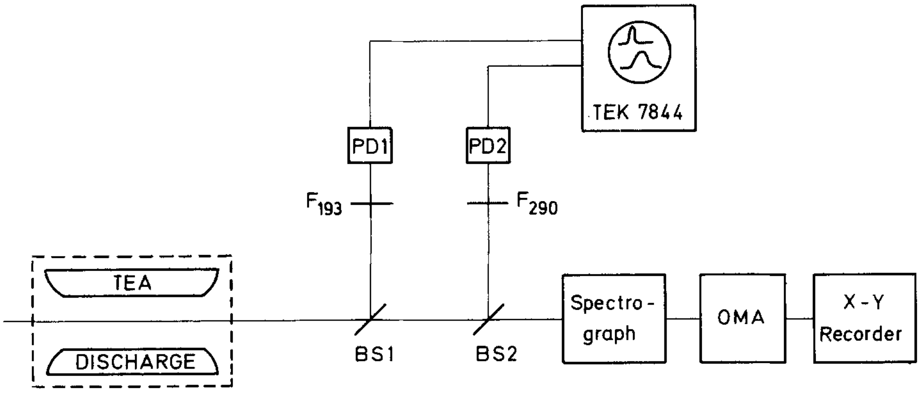

Fig. 1. Experimental arrangement. (BS: beamsplitters; F: narrow band filters; PD: photodiodes)

Gas pressures were varied within the ranges 0.05–6 mbar for F_2, 50–3800 mbar for He, and 50–2500 mbar for Ar. Ratios He : Ar varied between 60 : 1 and 1 : 2. Total pressure was $\leqq 4000$ mbar.

Time integrated spectra were recorded using a spectrograph in conjunction with a uv-sensitized OMA system (B+M Spektronik, Model OSA 500 equipped with scintillator). Time resolved measurements of Ar_2F^* and ArF^* emissions were made using fast photodiodes (Hamamatsu R 617 S-5) connected to a dual beam scope (TEK 7844). In this case, discrimination between ArF^* (193 nm) and Ar_2F^* (290 nm) was achieved by narrow band filters.

2. The Formation of Ar_2F^*

Before presenting our results it seems appropriate to establish a basis for their interpretation by briefly listing some of the processes that can possibly result in the formation of the laser active species from $He/Ar/F_2$ mixtures.

Excited and ionized Ar which initiates the formation process may either be generated directly (electron impact) or via collisions involving He^* and He_2^*:

$$He^* + Ar \rightarrow Ar^* + He, \qquad (1)$$

$$He_2^* + Ar \rightarrow Ar^* + 2\,He, \qquad (2)$$

$$He^* + Ar \rightarrow He + Ar^+ + e^-, \qquad (3)$$

$$He_2^* + Ar \rightarrow 2\,He + Ar^+. \qquad (4)$$

Reaction (1) proceeds slowly [10] compared to processes (2–4) [10, 17, 18].

Both excited and ionized Ar atoms are channelled into the excited dimer state via the following termolecular reactions:

$$Ar^+ + Ar + He \rightarrow Ar_2^+ + He, \qquad (5)$$

$$Ar^+ + 2\,Ar \rightarrow Ar_2^+ + Ar, \qquad (6)$$

$$Ar^* + Ar + He \rightarrow Ar_2^* + He, \qquad (7)$$

$$Ar^* + 2\,Ar \rightarrow Ar_2^* + Ar. \qquad (8)$$

ArF^* formation is considered to occur via ion-ion recombination:

$$Ar_2^+ + F^- \rightarrow ArF^* + Ar, \qquad (9)$$

$$Ar^+ + F^- + (M) \rightarrow ArF^* + (M) \qquad (10)$$

(where M is an arbitrary collision partner) and/or by formation reactions like [10]:

$$Ar^* + F_2 \rightarrow ArF^* + F. \qquad (11)$$

Finally, these excited and ionized dimers participate in reactions resulting in the formation of the trimer Ar_2F^*:

$$ArF^* + Ar + Ar \xrightarrow{k_1} Ar_2F^* + Ar, \qquad (12)$$

$$ArF^* + Ar + He \xrightarrow{k_2} Ar_2F^* + He, \qquad (13)$$

$$Ar_2^* + F_2 \xrightarrow{k_3} Ar_2F^* + F, \qquad (14)$$

$$Ar_2^+ + F^- + (M) \xrightarrow{k_4} Ar_2F^* + (M). \qquad (15)$$

Figure 2, in a simplified form, visualizes the formation mechanism for ArF^* and Ar_2F^*, as it is suggested by (5–15).

The rate equation describing the mechanism of formation of Ar_2F^* can thus be written

$$\begin{aligned}\frac{d}{dt}[Ar_2F^*] = {}& k_1[ArF^*][Ar]^2 + k_2[ArF^*][Ar][He] \\ & + k_3[Ar_2^*][F_2] \\ & + k_4[F^-][Ar_2^+][M] - \frac{[Ar_2F^*]}{\tau}. \qquad (16)\end{aligned}$$

τ is the effective exponential decay constant of Ar_2F^*. It is given by

$$\begin{aligned}\tau^{-1} = {}& \tau_{290}^{-1} + k_5[F_2] + k_6[Ar] + k_7[He] + k_8[Ar]^2 \\ & + k_9[He]^2 + k_{10}[Ar][He]. \qquad (17)\end{aligned}$$

Here τ_{290} is the radiative lifetime of Ar_2F^* and k_i are rate constants for the quenching of Ar_2F^* by the species shown in square brackets.

3. Results and Analysis

From the time resolved measurements of the ArF^* and Ar_2F^* fluorescence two observations can be made (Fig. 3):

1) Ar_2F^* emission reaches its maximum only after ArF^* has peaked and dropped to a very low value again. This supports the assumption of ArF^* being a precursor of the trimer, as it has also been suggested by Marowsky et al. [8].

2) The Ar_2F^* trace appears to be a superposition of two events peaking at different times. The decay does not show simple exponential behavior. This seems to suggest that this molecule has more than just one precursor, the fast and slow decay rates reflecting mechanisms of formation on two different time scales. We see evidence that ArF^* is responsible for the fast formation but, at this point, hesitate to speculate on the detailed nature of the slow reaction. This reaction must be slow on the timescale of the Ar_2F^* lifetime, otherwise we would not observe a second, distinct peak. It is conceivable that it involves slow energy transfer processes and ion-ion recombinations.

If the Ar pressure is raised from 800 mbar (Fig. 3) to 2000 mbar (Fig. 4), the relative contributions from different pathways change drastically. The second component of the Ar_2F^* emission that only began to appear at $p_{Ar} = 800$ mbar now clearly dominates in the overall signal. At the same time, the appearance of the second peak is further delayed relative to the first one. From Fig. 4 we obtain an exponential decay rate for the second peak of ~500 ns.

Variation of the He pressure has only minor influence on the fluorescence signal. This indicates that contributions from reactions (1–4) are of lesser importance.

Increasing the number density of Ar atoms facilitates dimerization reactions (5–8). In view of the comparatively low electron temperatures in the discharge, reactions proceeding via ionic channels (5 and 6) will likely be of minor importance. The increased supply of the Ar_2^* species will then greatly enhance the contribution from (14). The influence from (15) should, again, not be very noticeable, for reasons outlined above.

We draw support for this resoning from a comparison with data obtained under e-beam excitation conditions (transverse and longitudinal geometries) where corresponding fluorescence intensity measurements do not reveal a second peak [4, 6, 11–13]. Due to high e-energies ionic channels (5, 6, 9, 10) will be dominant

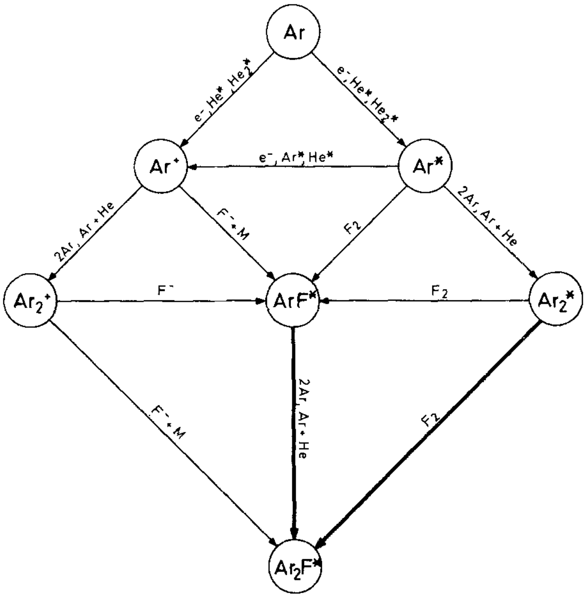

Fig. 2. Simplified scheme describing the formation of Ar_2F^*. Arrows mark reaction steps in which the shown collision partners are involved

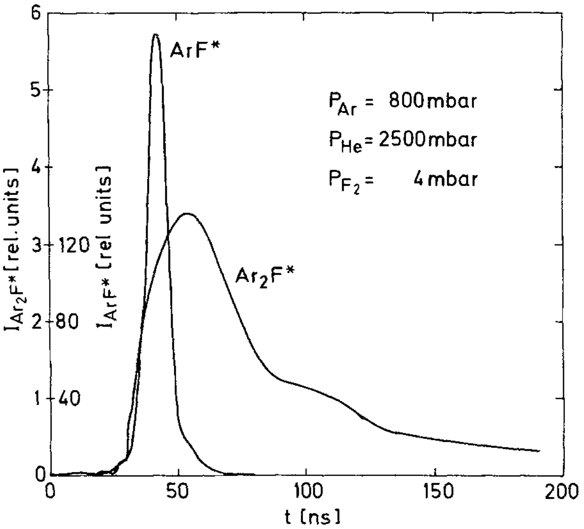

Fig. 3. Time-resolved fluorescence intensity of ArF^* and Ar_2F^*

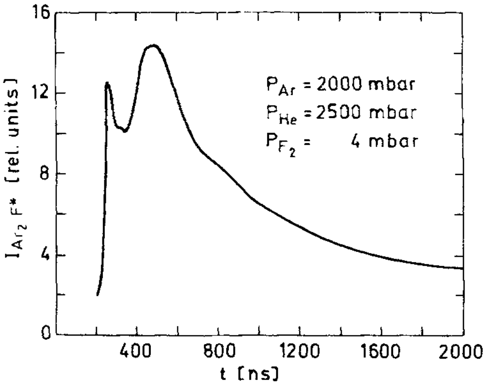

Fig. 4. Time-resolved fluorescence intensity of Ar_2F^*. Compared to Fig. 3, this graph demonstrates the effect of an increased Ar pressure

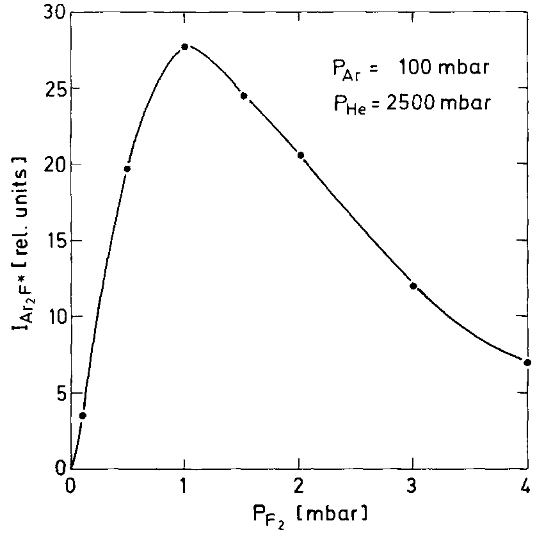

Fig. 5. Peak intensity of Ar_2F^* fluorescence vs. F_2 pressure. Ar and He partial pressures were kept constant

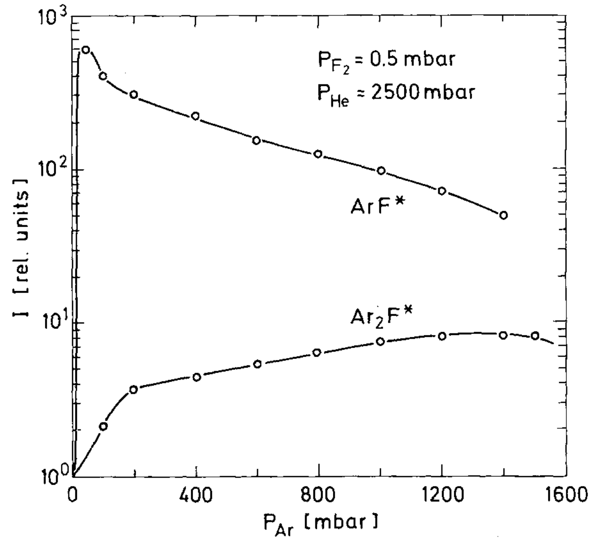

Fig. 6. Ar pressure dependence of the Ar_2F^* and ArF* fluorescence intensity (peak value)

and the preferred route of Ar_2F^* formation will be via ArF*, (12, 13).

The observation of a second peak obtained in a coaxial e-beam geometry [8, 9] at Ar pressures higher than the ones of this experiment, does not necessarily obsolete this reasoning: Once the electrons have penetrated the wall of the tubular anode containing the laser gas they are confined in a potential that supports oscillatory motions, which results in a rapid loss of energy due to multiple collisions. The electron temperatures of the coaxial geometry are thus considerably lower than those in the transverse arrangement. This seems to justify the comparison of coaxial excitation with TEA discharge data.

The Ar_2F^* emission shows a pronounced peak as the F_2 pressure is varied (Fig. 5). From the decay rates that we obtained for various F_2 pressures we derived the quenching rate constant $k_5 = 1.83 \times 10^{-10}\,\mathrm{cm^3\,s^{-1}}$, cf. (17). These data were taken at an Ar pressure sufficiently low to suppress the second, slowly decaying component. We assume that under the conditions pertinent to this experiment three body collisions may be neglected. Quenching rates k_6 and k_7, describing the effects of two body collisions with Ar and He, respectively, have been determined to be: $k_6 = 2.2 \times 10^{-14}\,\mathrm{cm^3\,s^{-1}}$ [8] and $k_7 = 0.5 \times 10^{-14}\,\mathrm{cm^3\,s^{-1}}$ [13]. Using these values, the Stern-Volmer plot yields a radiative lifetime for Ar_2F^* of $\tau_{290} = 236$ ns.

Considering the magnitude of k_6, quenching due to Ar should be a minor loss mechanism. The formation reactions (12) and (13) would thus suggest that, by increasing the Ar pressure, we might obtain higher Ar_2F^* intensities at the expense of ArF* output. Figure 6, which compares the intensities of both species verifies this expectation.

4. Conclusion

The excitation of $He/Ar/F_2$ mixtures in a TEA discharge results in the formation of ArF* as well as Ar_2F^* molecules. The production of Ar_2F^* proceeds via two routes on largley different timescales. The fast formation suggests the participation of ArF* in a termolecular reaction (12, 13) to yield the excited trimer. The slow process indicates a reaction involving Ar_2^* (14) via Ar* (8) and/or, possibly, other slow intermediate steps. The relative contributions from both sources can be controlled by varying the ratio of rare gas pressures. This paramater also controls the relative signal strengths observed at 193 and 290 nm. Information on the slow reaction step should be obtained from additional measurements of time-resolved Ar_2^* emission in vuv.

This experiment tried to evaluate the prospects of realizing a discharge pumped Ar_2F^* laser. The parameters that maximize the fluorescence emission of this trimer could be determined. However, the details of various quenching mechanisms that may prevent the buildup of sufficient gain for laser action are still in the dark: The mechanism of formation is very complex as it involves many transitory species whose absorptive characteristics are not known. We therefore suggest to gather corresponding data and measure the transient absorption around 290 nm. Quenching of Ar_2F^* by electrons [20] has also been invoked and merits attention.

Acknowledgements. The authors wish to thank W. Schmid, P. Hering for their valuable discussions and suggestions. Thanks are due to H. Bauer, M. Fischer, and G. Brandl for technical assistance.

References

1. J.E. Velazco, D.W. Setser: IEEE J. QE-**11**, 708 (1975)
2. J.E. Velazco, D.W. Setser: J. Chem. Phys. **62**, 1990 (1975)
3. W.R. Wadt, P.J. Hay: Appl. Phys. Lett. **30**, 573 (1977)
4. D.C. Lorents, R.M. Hill, D.L. Huestis, M.V. McCusker, H.H. Nakano: In *Electronic Transition Lasers II*, ed. by L.E. Wilson, S.N. Suchard, J.I. Steinfeld (MIT, Cambridge, MA 1977)
5. D.C. Lorents, D.L. Huestis, M.V. McCusker, H.H. Nakano, R.M. Hill: J. Chem. Phys. **68**, 15 (1978)
6. H.H. Nakano, R.M. Hill, D.C. Lorents, D.L. Huestis, M.V. McCusker: Stanford Research Institute Technical Report No. MP 76–99 (1976)
7. N.G. Basov, V.A. Nanilychev, V.A. Dolgikh, O.M. Kerimov, V.S. Lebedev, A.G. Molchanov: JETP Lett. **26**, 16 (1977)
8. G. Marowsky, G.P. Glass, F.K. Tittel, K. Hohla, W.L. Wilson, H. Weber, IEEE J. QE-**18**, 898 (1982)
9. H. Weber, K. Hohla: Private communication (unpublished)
10. Ch. K. Rhodes (ed.): *Excimer Lasers* (Springer, Berlin, Heidelberg, New York 1979) p. 88
11. C.H. Chen, M.G. Payne: Appl. Phys. Lett. **32**, 358 (1978)
12. C.H. Chen, M.G. Payne, J.P. Judish: J. Chem. Phys. **69**, 1626 (1978)
13. N. Böwering, R. Sauerbrey, H. Langhoff: Unpublished
14. M. Diegelmann, H.P. Grieneisen, K. Hohla, Xue-Jing Hu, J. Krasinski, K.L. Kompa: Appl. Phys. **23**, 283 (1980)
15. D.C. Lorents, D.L. Huestis, M.V. McCusker, H.H. Nakano, R.M. Hill: J. Chem. Phys. **68**, 4657 (1978)
16. C.H. Chen, J.P. Judish, M.G. Payne: J. Phys. B **11**, 2189 (1978)
17. A. Gedanken, J. Jortner, B. Raz, A. Szöke: J. Chem. Phys. **57**, 3456 (1972)
18. D.K. Bohme, N.G. Adams, M. Mosesman, D.B. Dunkin, E.E. Ferguson: J. Chem. Phys. **52**, 5094 (1970)
19. C.H. Chen, M.G. Payne: IEEE J. QE-**15**, 149 (1979)
20. K.S. Jancaitis, H.T. Powell: 34th Annual Gaseous Electronics Conference (October 20–23, 1981) Paper FB 9